Electronic Supplementary Material

Encapsulation of polyethylene glycol in cellulose-based porous capsules for latent heat storage and light-to-thermal conversion

Jiangwei Li, Lina Meng, Jiaxuan Chen, Xu Chen, Yonggui Wang (✉), Zefang Xiao, Haigang Wang, Daxin Liang, Yanjun Xie (✉)

Key Laboratory of Bio-based Material Science and Technology (Ministry of Education), College of Material Science and Engineering, Northeast Forestry University, Harbin 150040, China

E-mails: wangyg@nefu.edu.cn (Wang Y); yxie@nefu.edu.cn (Xie Y).

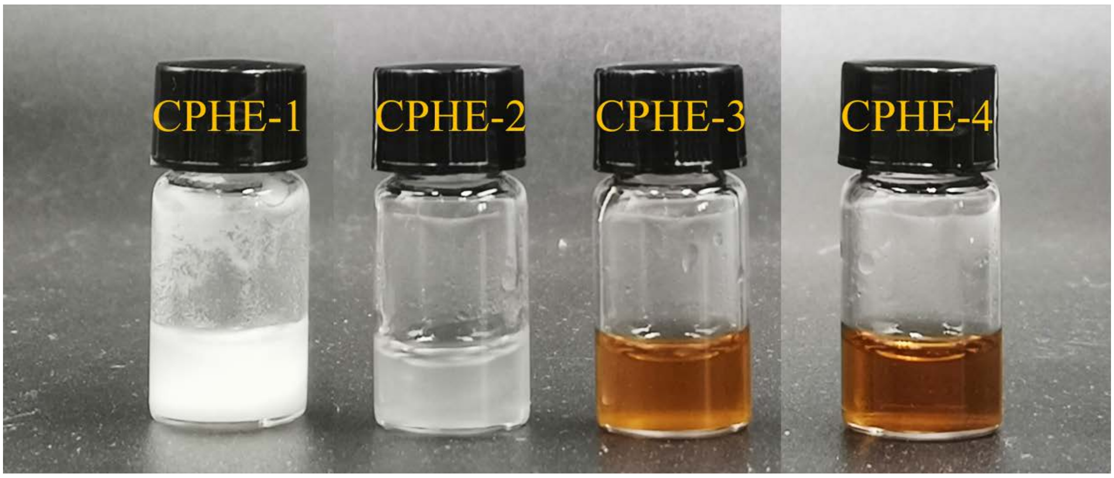

Figure S1. Photos of CPHEs in water.

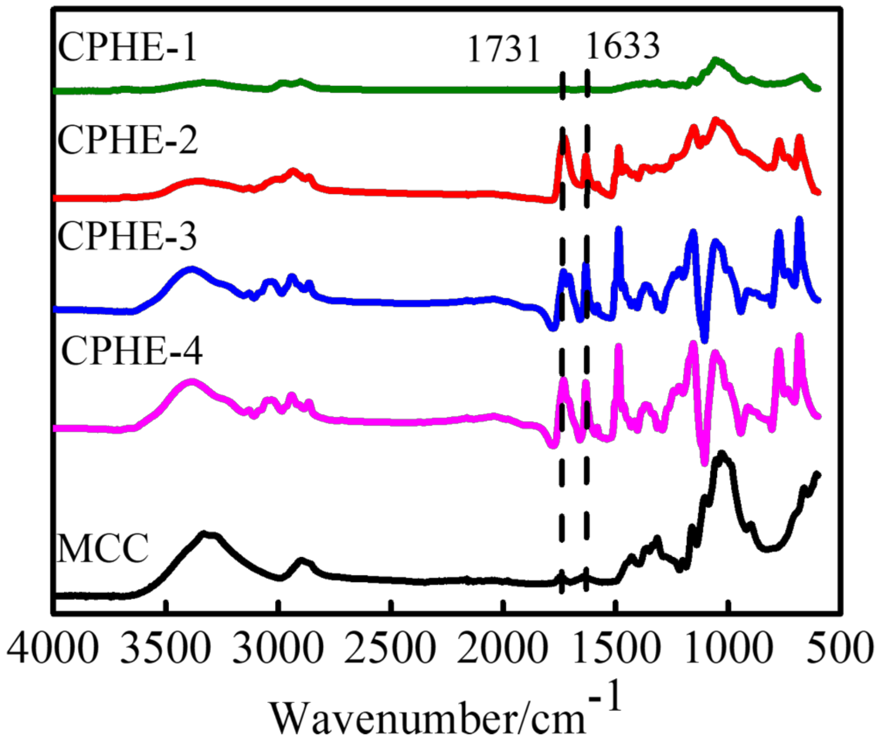

Figure S2. FTIR spectra of CPHEs and MCC.

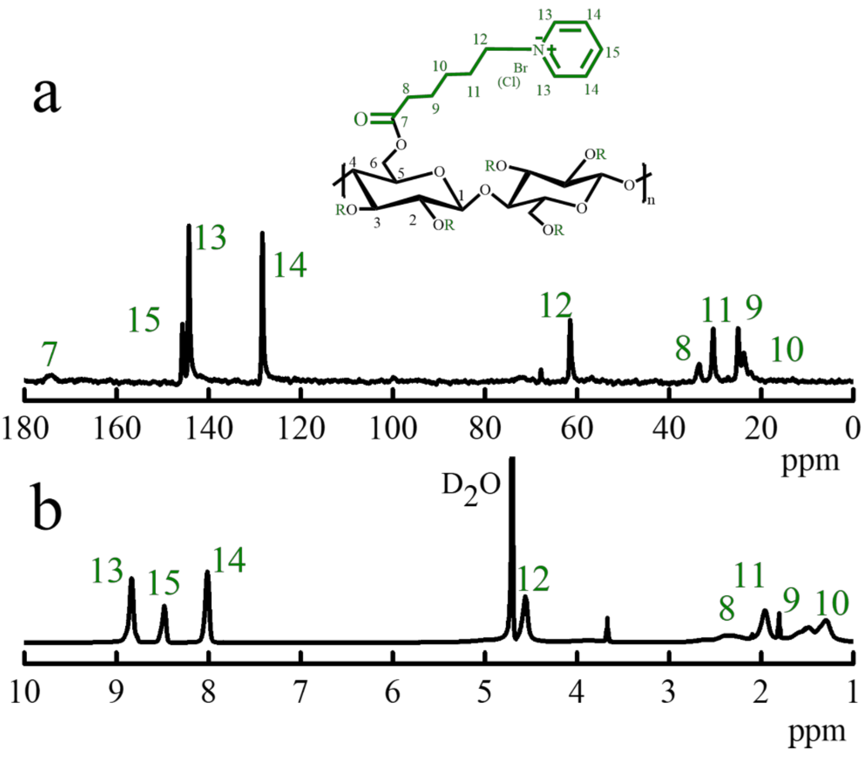

Figure S3. (a) Liquid-state ^{13}C and (b) Liquid -state ^{1}H NMR spectra of CPHE-4.

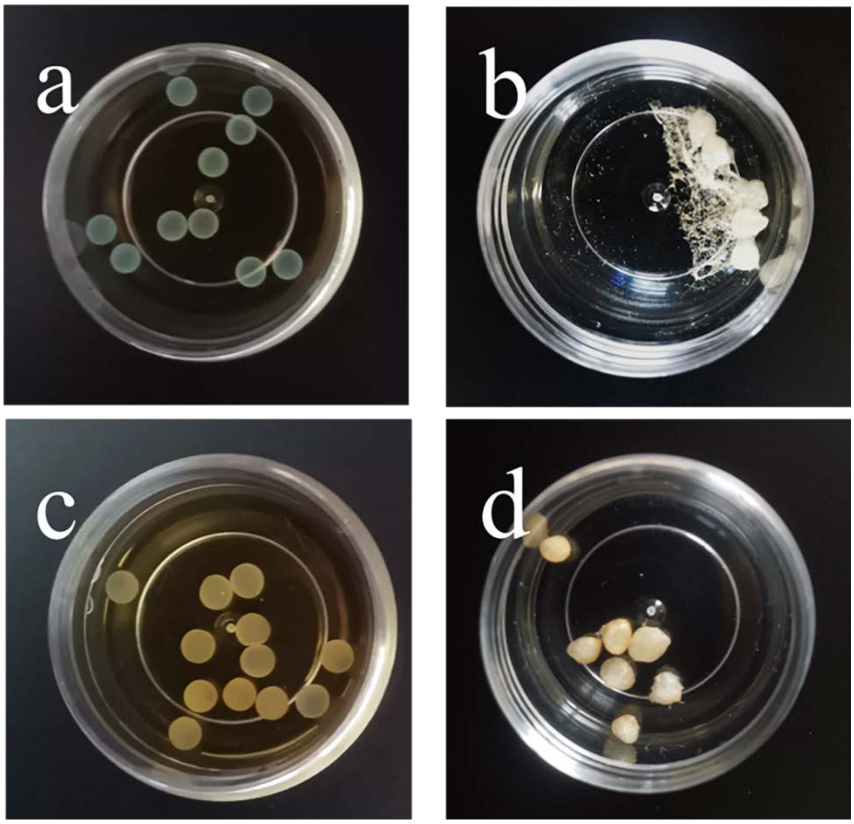

Figure S4. Photos of CPEC capsules, (a-b) without Fe^{3+} addition and (c-d) Fe^{3+} addition.

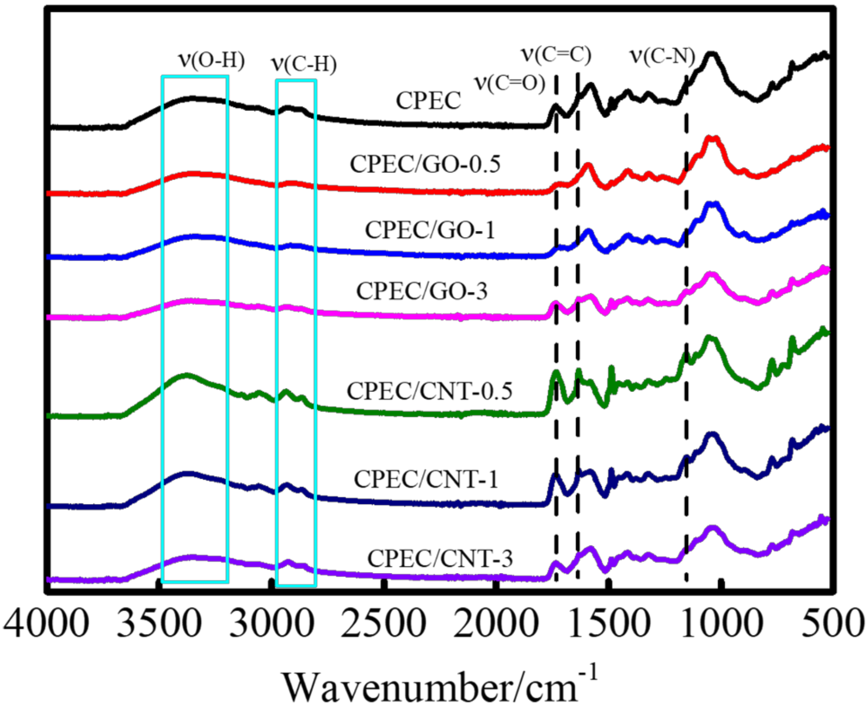

Figure S5. FTIR spectra of all capsules.

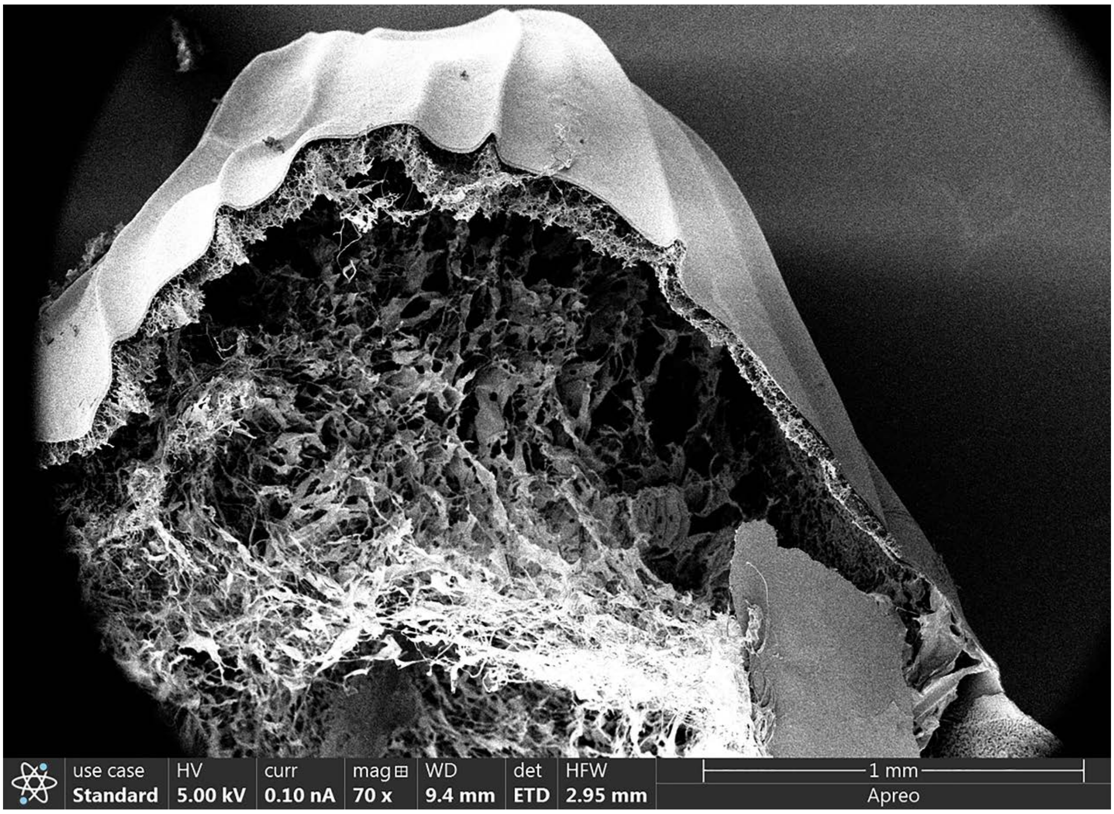

Figure S6. SEM images of core-shell structure of CPEC capsules.

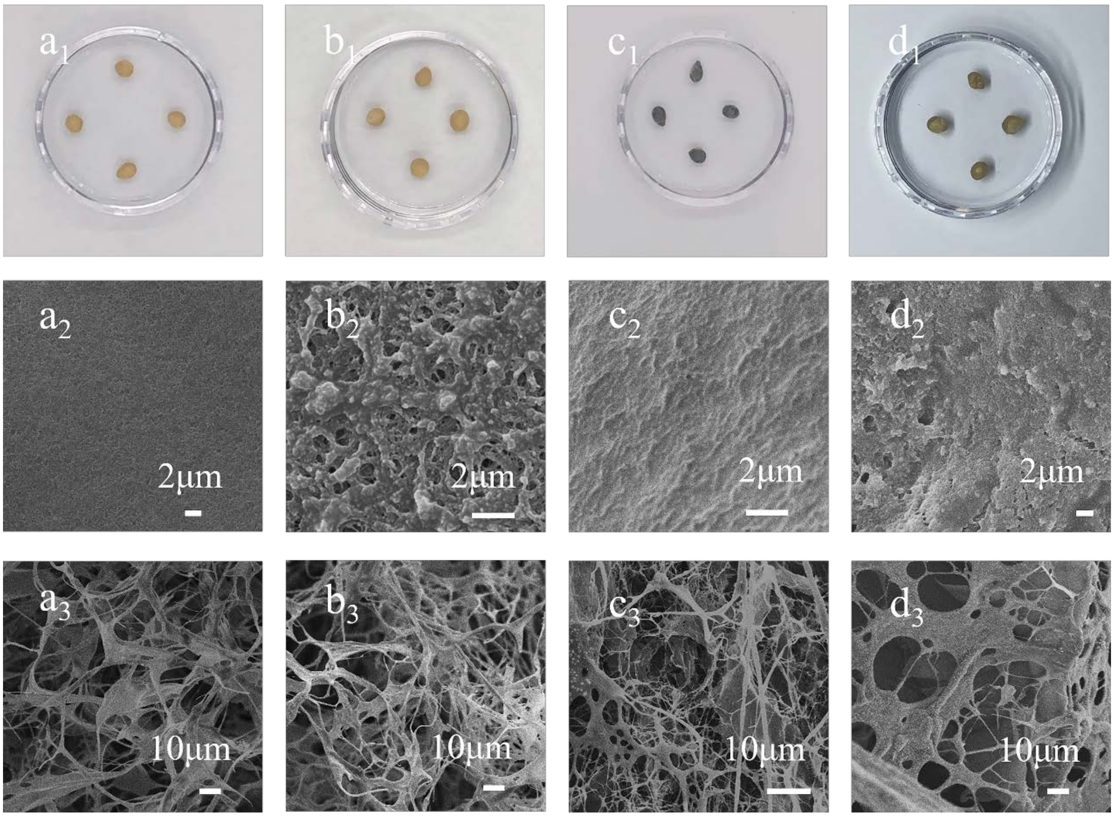

Figure S7. (a_1-d_1) Photos of (a_1) CPEC/GO-0.5, (b_1) CPEC/GO-1, (c_1) CPEC/CNT-0.5, (d_1)

CPEC/CNT-1. (a_2-d_2) SEM images of the surface structure of (a_2) CPEC/GO-0.5, (b_2) CPEC/GO-1, (c_2) CPEC/CNT-0.5, (d_2) CPEC/CNT-1. (a_3-d_3) SEM images of the inner structure of (a_3) CPEC/GO-0.5, (b_3) CPEC/GO-1, (c_3) CPEC/CNT-0.5, (d_3) CPEC/CNT-1.

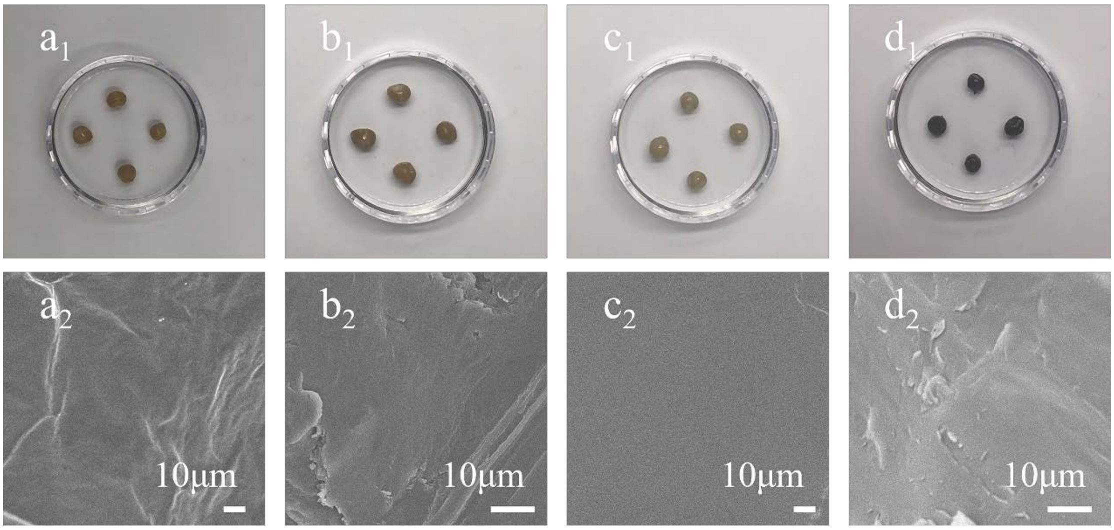

Figure S8. (a_1-d_1) Photos of (a_1) PEG@CPEC/GO-0.5, (b_1) PEG@CPEC/GO-1, (c_1) PEG@CPEC/CNT-0.5, (d_1) PEG@CPCE/CNT-1. (a_2-d_2) SEM images of (a_2) PEG@CPEC/GO-0.5, (b_2) PEG@CPEC/GO-1, (c_2) PEG@CPEC/CNT-0.5, (d_2) PEG@CPCE/CNT-1.

Table S1. Comparison of PEG loading rate of the PEG-based composite PCMs.

PEG-based composite PCMs	Loading rate /%	References
Cellulose nanofiber/graphene nanoplatelet hybridcoated melamine foam/PEG	95.2	[1]
MXene aerogel/PEG	90	[2]
Graphene/carbon nanotube aerogel/PEG	98.8	[3]
Cellulose/graphene aerogel/PEG	1166	[4]
Polyimide/phosphorene/PEG	4067	[5]
Lignin-based hierarchical porous carbon/PEG	85	[6]

SA/PEG	93	[7]
Nano-aluminosilicate/PEG	77.5	[8]
Expanded dickite/PEG	179.3	[9]
Cellulose/graphene aerogel/PEG	4321	[10]
CA/PEG	96.5	[11]
Cellulose -based porous capsule/PEG	3433	This cork

The loading rates (R_L) of PEG were calculated by the following equation [10]:

$$R_L = \frac{\mathrm{m} - m_0}{m_0} * 100\%$$

Where m_0 is the initial mass of the capsules, and m is the final mass of the composite PCMs.

Table S2. Thermal reliability of prepared samples after1, 50, 100, 150 and 200 thermal cycles.

	Melting process		Crystallization process	
	T_m /°C	H_m / J g^{-1}	T_c /°C	H_c /J g^{-1}
PEG@CPEC 1 cycle	65.41	139.5	42.51	136.9
PEG@CPEC 50 cycle	65.20	139.4	43.37	135.7
PEG@CPCE 100 cycle	62.17	136.9	43.12	125.9
PEG@CPEC 150 cycle	68.28	135.0	41.11	125.1
PEG@CPEC 200 cycle	66.18	129.9	40.16	124.4
PEG@CPCE/GO-3 1 cycle	65.47	142.2	42.32	137.4
PEG@CPCE/GO-3 50 cycle	65.70	131.2	42.63	123.9
PEG@CPCE/GO-3 100 cycle	64.41	129.5	43.46	122.9
PEG@CPCE/GO-3 150 cycle	65.88	125.3	40.01	122.4
PEG@CPCE/GO-3 200 cycle	64.49	122.1	40.97	118.6

PEG@CPEC/CNT-3 1 cycle	64.98	138.6	42.67	131.2
PEG@CPCE/CNT-3 50 cycle	65.19	129.6	43.40	126.4
PEG@CPEC/CNT-3 100 cycle	63.82	125.3	43.71	121.6
PEG@CPCE/CNT-3 150 cycle	65.19	123.5	39.57	120.4
PEG@CPEC/CNT-3 200 cycle	63.82	119.1	40.50	107.2

Table S3. Thermal conductivity of prepared CPEC, CPEC/GO-3, CPEC/CNT-3 porous capsules.

Samples	Thermal conductivity /W m^{-1}*K^{-1}
CPEC	0.0389
CPEC/GO-3	0.0404
CPEC/CNT-3	0.0424

References

1. Wu H, Deng S, Shao Y, Yang J, Qi X, Wang Y. Multiresponsive Shape-Adaptable Phase Change Materials with Cellulose Nanofiber/Graphene Nanoplatelet Hybrid-Coated Melamine Foam for Light/Electro-to-Thermal Energy Storage and Utilization. ACS Applied Materials & Interfaces, 2019, 11(50): 46851-46863
2. Lin P, Xie J, He Y, Lu X, Li W, Fang J, Yan S, Zhang L, Sheng X, Chen Y. MXene aerogel-based phase change materials toward solar energy conversion. Solar Energy Materials and Solar Cells, 2020, 206: 110229
3. Cao Q, He F, Li Y, He Z, Fan J, Wang R, Hu W, Zhang K, Yang W. Graphene-carbon nanotube hybrid aerogel/polyethylene glycol phase change composite for thermal management. Fullerenes, Nanotubes and Carbon Nanostructures, 2020, 28(8): 656-662
4. Yang J, Zhang E, Li X, Zhang Y, Qu J, Yu Z-Z. Cellulose/graphene aerogel supported phase change composites with high thermal conductivity and good shape stability for thermal energy storage. Carbon, 2016, 98: 50-57
5. Zheng Z, Shi T, Liu H, Wu D, Wang X. Polyimide/phosphorene hybrid aerogel-based composite phase change materials for high-efficient solar energy capture and photothermal conversion. Applied Thermal Engineering, 2022, 207: 118173
6. Li T, Pan H, Xu L, Ni K, Shen Y, Li K. Shape-stabilized phase change material with high phase change enthalpy made of PEG compounded with lignin-based carbon. International

Journal of Biological Macromolecules, 2022, 213: 134-144
7. Liu L, Fan X, Zhang Y, Zhang S, Wang W, Jin X, Tang B. Novel bio-based phase change materials with high enthalpy for thermal energy storage. Applied Energy, 2020, 268: 114979
8. Zhen L, Meng G, Zhou B, Ma W, Yang Y, Duan X, Fu Y, Wang H. Efficient utilization of interparticle mesopores in aluminosilicate towards thermal energy storage. Journal of Energy Storage, 2021, 36: 102359
9. Su H, Ding M, Yang K, Li Y, Zhang Z, Li F, Xue B. Properties and characterization of novel expanded dickite based composite phase change material. Journal of Applied Polymer Science, 2022, 139(21): e52197
10. Du X, Zhou M, Deng S, Du Z, Cheng X, Wang H. Poly(ethylene glycol)-grafted nanofibrillated cellulose/graphene hybrid aerogels supported phase change composites with superior energy storage capacity and solar-thermal conversion efficiency. Cellulose, 2020, 27(8): 4679-4690
11. Sundararajan S, Samui A B, Kulkarni P S. Shape-stabilized poly(ethylene glycol) (PEG)-cellulose acetate blend preparation with superior PEG loading via microwave-assisted blending. Solar Energy, 2017, 144: 32-39